Macromolecules

Article

pubs.acs.org/Macromolecules

Co-Nonsolvency of Poly(*n*-isopropylacrylamide) in Deuterated Water/Ethanol Mixtures

Michael J. A. Hore* and Boualem Hammouda*

National Institute of Standards and Technology Center for Neutron Research, 100 Bureau Drive, Gaithersburg, Maryland 20899-6102, United States

Yuyan Li and He Cheng*

State Key Laboratory of Polymer Physics & Chemistry, The Institute of Chemistry, Chinese Academy of Sciences, Beijing, China, 100190

ABSTRACT: Small-angle neutron scattering was used to investigate poly(*N*-isopropylacrylamide) (PNIPAM) polymer solutions in *d*-water/*d*-ethanol mixtures. A wide poor-solvent region was observed for mixtures near 60% *d*-water/40% *d*-ethanol mixture. Spinodal lines were determined, permitting a mapping of the mixing/demixing regions of the phase diagram which comprises two main branches: the left branch (with mostly *d*-ethanol) where phase separation occurs upon cooling (UCST) and the right branch (with mostly *d*-water) where phase separation occurs upon heating (LCST). The ternary random phase approximation model was used to analyze SANS data. Three Flory–Huggins interaction parameters (PNIPAM/*d*-water, PNIPAM/*d*-ethanol and *d*-water/*d*-ethanol) were obtained. These display the reassuring $1/T$ behavior but show strong dependence on *d*-water/*d*-ethanol fraction. The conformation of polymer chains was determined by monitoring of the radius of gyration. Chains tend to swell with increasing temperature except close to the boundary of the left branch of the phase diagram (40% *d*-water) where they are observed to shrink.

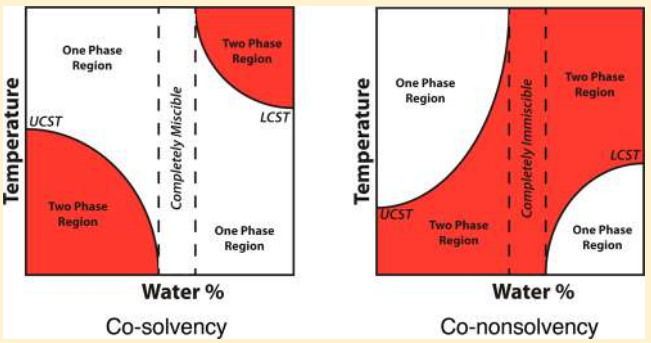

INTRODUCTION

Mixing solvents can either enhance or decrease the solvation of polymers. Most water-soluble polymers dissolve better in solvent mixtures (cosolvency). For example, poly(ethylene oxide) (PEO) dissolves well in ethanol and in water and dissolves even better in ethanol/water mixtures. Semidilute PEO solutions in ethanol phase separate upon cooling; they obey an upper critical solution temperature (UCST) phase behavior. On the other hand, semidilute PEO solutions in water phase separate upon heating; they obey a lower critical solution temperature (LCST) phase behavior. When dissolved in ethanol/water mixtures, PEO follows an interesting phase diagram characterized by a transition from UCST to LCST as the water fraction in the binary solvent mixture increases. The transition region between these two limits shows no hint of phase transition and is "perfectly" mixed over a wide temperature range.[1]

A small number of polymers follow the cononsolvency phase behavior wherein their solubility in a mixture of good solvents decreases or even vanishes. For example, polystyrene dissolves in cyclohexane and *N*,*N*-dimethylformamide (DMF), but is largely immiscible in mixtures of the two.[2] Other polymers, such as poly(ether imide), poly(vinylpyrrolidone), and poly(vinyl alcohol) also exhibit cononsolvency behavior in certain solvent combinations.[3−5] Poly(*N*-isopropylacrylamide) (PNIPAM) is one of the most studied water-soluble polymers which displays cononsolvency behavior in binary mixtures of several solvents, such as water and ethanol.[2,3] PNIPAM has been investigated extensively due in part to its thermoresponsive properties in aqueous solutions. While a large amount of attention has been devoted to PNIPAM-based gels, relatively few studies have constructed phase diagrams of PNIPAM homopolymer solution in mixed solvents.

PNIPAM exhibits cononsolvency behavior in mixtures of water and methanol. While evidence of cononsolvency behavior was seen as early as 1987,[6] some of the first studies of PNIPAM solutions are due to Schild et al.[7] and Winnik et al.,[8] who observed that PNIPAM precipitated in equal volume mixtures of water and methanol. Zhang and Wu[9] studied the chain collapse of individual PNIPAM chains in mixtures of water and methanol using laser light scattering (LLS) and observed a coil-to-globule transition of the chains as the methanol content in

Received: August 8, 2013
Revised: September 9, 2013

 © XXXX American Chemical Society dx.doi.org/10.1021/ma401665h | *Macromolecules* XXXX, XXX, XXX–XXX

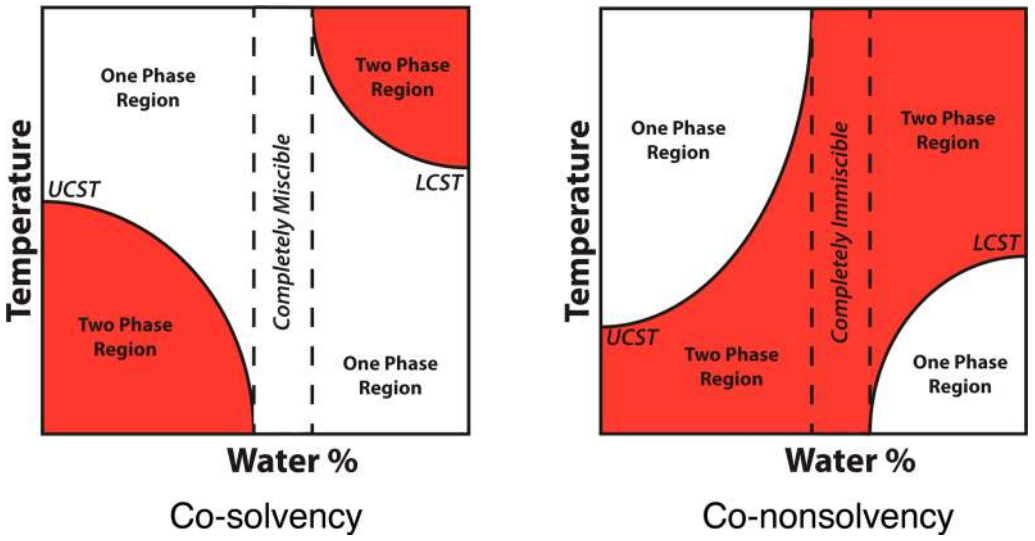

Figure 1. Schematic representation of cosolvency (left) and cononsolvency (right) of polymers in mixed water/ethanol mixtures, showing variation of the phase transition line (UCST or LCST) between the mixed (one-phase) and demixed (two phase) regions with increasing water fraction in water/ethanol mixtures.

the solution increased between 17 mol % to 50 mol %. As methanol was added in excess of 50 mol %, the polymer globules expanded and the chains regained a coil conformation. Tucker and Stevens[10] observed similar coil-to-globule transition using atomistic molecular dynamics simulations of PNIPAM oligomers in water.

Costa and Freitas[11] studied the phase behavior of PNIPAM in solvent mixtures by measuring the cloud points of the solutions as the composition of the mixture varied. For water/methanol mixtures, they observed LCST behavior, with a spinodal temperature that decreased as methanol was added up to approximately 35 mol %, and then increased as additional methanol was added. The decrease in spinodal temperature for moderate amounts of methanol is indicative of decreased PNIPAM solubility in the solution. A similar LCST behavior was observed for water/acetone mixtures, where the spinodal temperature decreased to a minimum at approximately 20 mol % acetone, and then increased as additional acetone was added. Costa and Freitas also observed a unique solvation behavior for PNIPAM in mixtures of water and ethanol, water and propanol, as well as water and dimethylformamide (DMF). As in the case of PEO/water/ethanol solutions, these solvent blends are characterized by UCST and LCST behavior in pure ethanol and water, respectively. However, the curvature (characterized by the second derivative with respect to water content) of the spinodal temperatures with respect to the fraction of water in the solvent is reversed from the case of PEO. This implies that the one-phase and two-phase regions of the phase diagram are reversed for PNIPAM as compared to PEO, and hence, a region exists in the phase diagram where PNIPAM is completely insoluble in the solvent mixture. Figure 1 shows this trend schematically in the case of a PEO-like polymer (left) and a PNIPAM-like polymer (right). Similar PNIPAM phase behavior has been observed in dimethyl sulfoxide (DMSO)/water mixtures.[12] On the basis of spectroscopic measurements, Yamauchi and Maeda attribute the UCST/LCST behavior of PNIPAM in DMSO/water mixtures to competitive hydrogen bonding between the DMSO, water, and PNIPAM molecules. A statistical mechanical theory proposed by Tanaka and co-workers, applied to methanol/water mixed solvent, supports the competitive hydrogen bonding hypothesis.[13]

Here, the technique of small-angle neutron scattering (SANS) is used to investigate cononsolvency of PNIPAM polymer in dilute deuterated-ethanol/deuterated-water mixtures as a function of deuterated water content and temperature. The SANS technique is sensitive to composition fluctuations making it a useful tool for mixing/demixing phase behavior investigations in polymer solutions. SANS is also valuable for conformation studies in polymer solutions.

EXPERIMENTAL SECTION

Polymer Synthesis. *N*-Isopropylacrylamide (NIPAM) (Sigma, 97%) was purified by recrystallization from a 1:3 mixture (by volume) of benzene and hexane. 2,2′-Azobis(isobutyronitrile) (AIBN) (Sigma, 98%) was recrystallized twice from hot water. Anhydrous dioxane, dichloromethane, and ethyl ether were used as received. *S*-1-Ethyl-*S*′-(α,α′-dimethyl-α″-acetic acid) trithiocarbonate (EDMAT) was synthesized according to the literature.[14]

RAFT polymerization was carried out at 65 °C in 50% mass fraction dioxane as previously reported.[15] EDMAT was used as a chain transfer agent (CTA) and AIBN was the initiator. In a typical RAFT procedure, NIPAM, EDMAT and AIBN([NIPAM]: [EDMAT]: [AIBN] = 350:1:0.1) was mixed in dioxane, and sealed in 20 mL glass vial equipped with a magnetic stirrer. It was degassed by three freeze−thaw cycles and then the vial was flame-sealed under vacuum. Polymerization was carried out at 65 °C for 3 h. The reaction was terminated by cooling, and the resultant product was diluted in dichloromethane and precipitated into anhydrous diethyl ether 3 times.

Sample Preparation. PNIPAM with M_n = 18 000 g/mol was used to prepare a series of 4% mass fraction PNIPAM solutions in *d*-ethanol, in *d*-water and in *d*-ethanol/*d*-water mixtures. Note that 4% PNIPAM fraction is well below the overlap concentration, and corresponds to the dilute regime. Deuterated solvents were used in order to enhance the neutron contrast. The series of prepared samples correspond to 0%, 10%, 20%, 30%, 40%, 50%, 60%, 70%, 80%, 90%, and 100% *d*-water in the *d*-water/*d*-ethanol mixture series. The low *d*-water and high *d*-water fraction samples dissolved well and were homogeneously mixed. The intermediate *d*-water (50%, 60% and 70%) samples did not dissolve within a reasonable temperature window and were therefore not measured.

dx.doi.org/10.1021/ma401665h | *Macromolecules* XXXX, XXX, XXX−XXX

Small-Angle Neutron Scattering (SANS). Measured temperatures were between 0 and 70 °C (every 10 °C) for the 0%, 10%, 20%, 30%, and 40% *d*-water fraction samples or between 0 and 35 °C (every 5 °C) for the 80%, 90%, and 100% *d*-water fractions. These sample conditions were guided by PNIPAM miscibility constraints. Note that the actual sample temperatures lagged slightly behind the set temperatures; for instance the 0 °C set temperature corresponds to 3 °C actual temperature, the 25 °C set temperature corresponds to 25 °C actual temperature and the 70 °C set temperature corresponds to 67 °C actual temperature.

SANS was performed on the 30 m NG3 instrument at the National Institute of Standards and Technology, Center for Neutron Research (NCNR, Gaithersburg, MD). SANS measurements were taken for two sample-to-detector distances of 1 and 4 m for the ethanol-rich solvent mixtures, and three sample-to-detector distances of 1, 4, and 13 m for the water-rich solvent mixtures. The neutrons had wavelengths of λ = 6 Å at the 1 and 4 m detector distances, and λ = 8.4 Å at the 13 m detector distance. The different wavelength at the 13 m detector position is due to the use of lenses to increase neutron flux on the sample. Standard data acquisition and data reduction techniques were employed to obtain radially averaged SANS data.

RESULTS

Small-Angle Neutron Scattering. Figures 2, 3, and 4 represent SANS data for 4% PNIPAM in pure *d*-ethanol (0% *d*-water), in 40% *d*-water/60% *d*-ethanol and in pure (i.e., 100%) *d*-water, respectively. This is typical scattering data for polymer solutions characterizing polymer/solvent interactions or "solvation" behavior. In *d*-ethanol, PNIPAM has a wide upper critical solution temperature (UCST) temperature window for mixing (Figure 2). The 40% *d*-water sample was also measured over a wide temperature window (Figure 3). The PNIPAM in pure *d*-water sample was measured over a limited temperature window (maximum temperature of 35 °C) since higher temperatures prompted lower critical solution temperature (LCST) demixing. Figure 4 shows the expected scattering from PNIPAM chains at intermediate and high values of *Q* (solvation feature), as well as the low-*Q* composition fluctuations (onset of phase separation) signal. Only the solvation feature is of interest here. Statistical error bars are comparable in size to the plotting symbols.

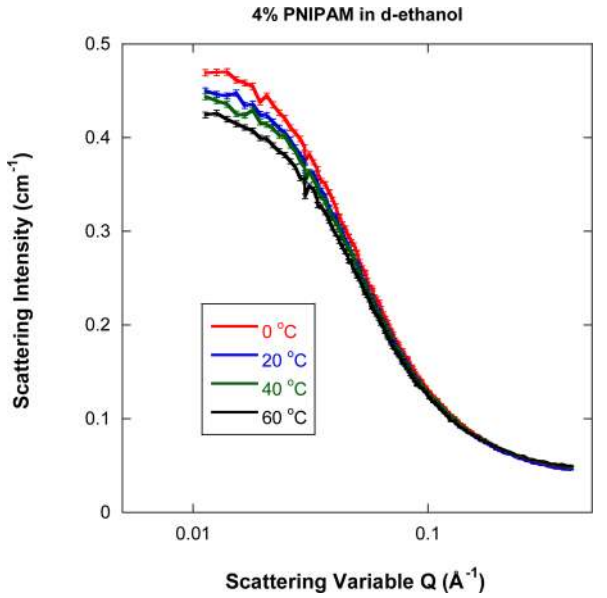

Figure 2. Scattering intensity for 4% PNIPAM in *d*-ethanol decreases for increasing temperature, showing UCST behavior. Statistical error bars correspond to one standard deviation.

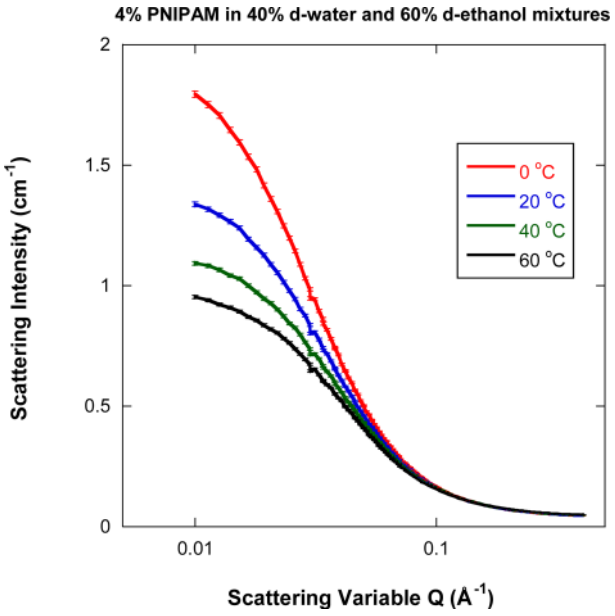

Figure 3. Scattering intensity for 4% PNIPAM in 40% *d*-water/60% *d*-ethanol for increasing temperature, showing UCST behavior. Statistical error bars correspond to one standard deviation.

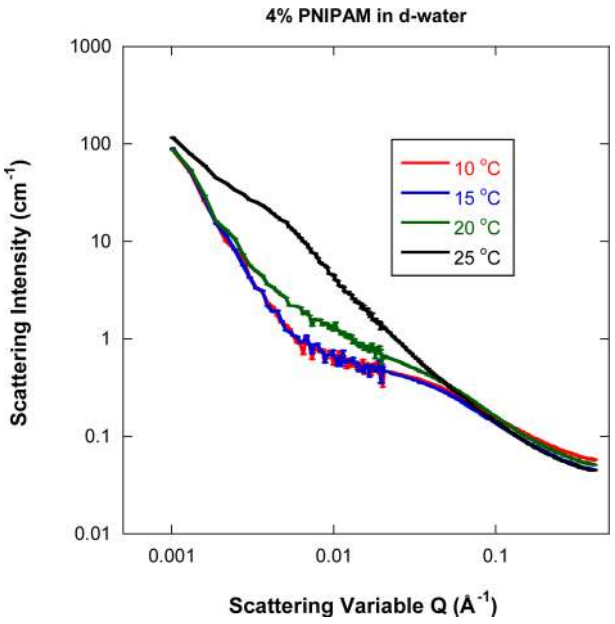

Figure 4. Scattering intensity for 4% PNIPAM in *d*-water increases for increasing temperature, showing LCST behavior. The low-Q onset of phase separation feature becomes dominant as temperature increases.

Phase Diagram. In order to determine the phase diagram for the 4% PNIPAM in *d*-water/*d*-ethanol mixtures, the scattering intensity in the thermodynamic (i.e., Q = 0) limit is needed. A simple empirical model is used to fit SANS data for samples with *d*-water fractions between 0% and 40%.

$$\frac{d\Sigma(Q)}{d\Omega} = \frac{C}{1 + (Q\xi)^m} + B \quad (1)$$

where $d\Sigma(Q)/d\Omega$ is the Q-dependent differential scattering cross section, C is the "solvation intensity", and B is the

dx.doi.org/10.1021/ma401665h | Macromolecules XXXX, XXX, XXX–XXX

incoherent scattering background due primarily to Q-independent scattering from hydrogen. ξ is a correlation length and m is the Porod exponent.

For samples with higher d-water fractions (between 80% and 100%), this model is used to fit the intermediate and high-Q data in addition to a power law model A/Q^n for the low-Q data representing composition fluctuations that get stronger as temperature increases. Nonlinear least-squares fits were performed for all SANS data and the fitting parameters were obtained for the various measured temperatures and d-water fraction samples. The parameters most relevant to demixing thermodynamics are the solvation intensity C, the correlation length ξ, and the high-Q Porod exponent m.

Plotting $1/C$ (inverse solvation intensity) for increasing $1/T$, where T is the absolute sample temperature, shows a linear behavior in the one phase region, as shown in Figure 5. A

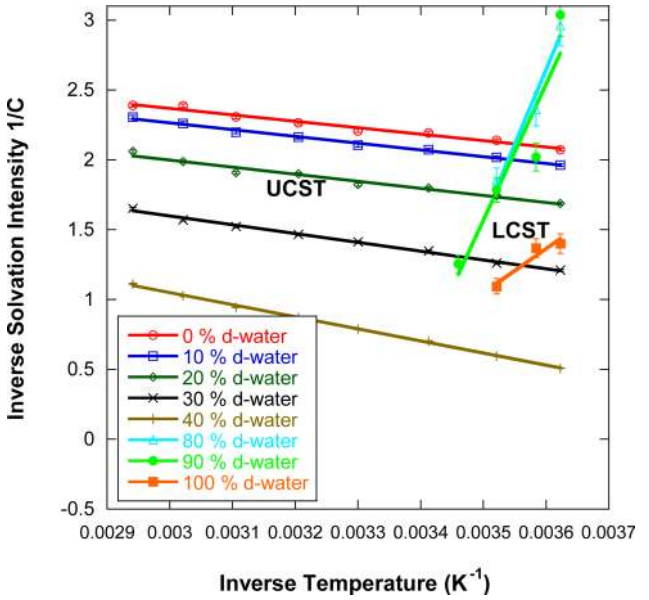

Figure 5. Variation of the inverse solvation intensity $1/C$ with inverse absolute temperature for 4% PNIPAM in various d-ethanol/d-water solvent mixtures. The UCST behavior is characterized by a negative slope while LCST is characterized by a positive slope. Statistical error bars correspond to one standard deviation.

negative slope represents the UCST behavior corresponding to low d-water fraction samples while a positive slope represents the LCST behavior corresponding to almost pure d-water fractions. Statistical error bars correspond to one standard deviation. Note that close to the pure d-water solvent limit, the low-Q signal due to the onset of phase separation merges with the intermediate-Q signal due to chain solvation so that it is not possible to determine the solvation intensity reliably especially for the high temperatures ($T \geq 25$ °C).

Extrapolation of this linear behavior (shown in Figure 5) to $1/C = 0$ from the mixed phase region yields an estimate for the spinodal temperature (reached when the solvation intensity C diverges). The extrapolated spinodal temperatures are plotted in Figure 6 across the various samples with different d-water fractions. The low d-water region (UCST behavior) and the high d-water fraction (LCST) region are well mapped out while the region in-between is only delineated. The 1-phase (mixed) and 2-phase (demixed) region are marked. The midregion is dominated by a wide demixing window centered around 60% d-

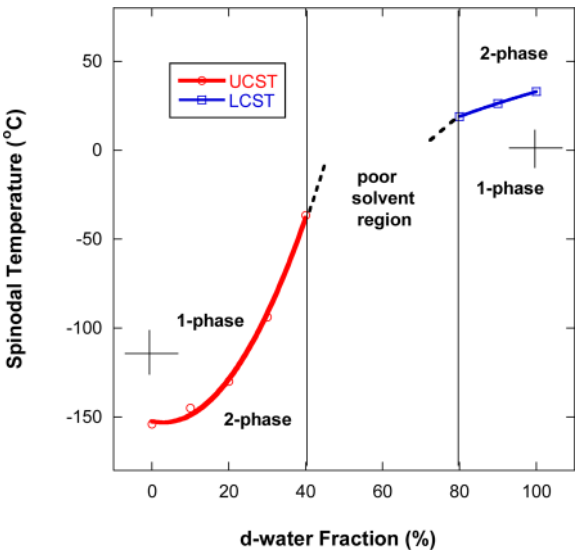

Figure 6. Variation of the UCST and LCST spinodal transition temperature lines for 4% PNIPAM solutions for increasing d-water fraction in d-ethanol/d-water solvent mixtures. The two freezing points are marked by crosses at the corners. Samples do not dissolve in the "poor solvent region" window.

water fraction. This corresponds to approximately 81.36 d-water molecules and 20.86 d-ethanol molecules for each PNIPAM monomer. The freezing points for pure d-ethanol (−114 °C) and pure deuterated water (1 °C) are marked with crosses at the corners. Note that the spinodal line in the left branch of the phase diagram obtained through the extrapolation procedure is below freezing while the right branch is above freezing.

Ternary Random Phase Approximation. The random phase approximation (RPA) model is used for an in-depth analysis of the SANS data. The RPA model has proven useful for investigations of the mixing/demixing thermodynamics of polymer mixtures. It is applied here to the ternary mixture of a polymer (PNIPAM) and two solvents (d-water and d-ethanol). It should be noted that this model is approximate.

The ternary RPA model[16,17] is described here briefly. The three components are defined as 1: PNIPAM, 2: d-water and 3: d-ethanol, the degrees of polymerization as n_1, n_2, and n_3, the volume fractions as ϕ_1, ϕ_2, and ϕ_3, and the specific volumes as v_1, v_2, and v_3 for the three components. The bare structure factors (when interactions are not included) are expressed as

$$S_{11}^0(Q) = n_1\phi_1 v_1 P(Q),\ S_{22}^0 = n_2\phi_2 v_2 \quad \text{and} \quad S_{33}^0 = n_3\phi_3 v_3 \tag{2}$$

$P(Q)$ is the polymer single-chain form factor described later, where the scattering variable $Q = (4\pi/\lambda)\sin(\theta/2)$. Note that the cross terms (S_{12}^0, etc.) do not contribute. The following parameters are defined:

$$V_{11} = \frac{1}{S_{33}^0} - \frac{2\chi_{13}}{v_{13}}$$

$$V_{22} = \frac{1}{S_{33}^0} - \frac{2\chi_{23}}{v_{23}}$$

$$V_{12} = \frac{1}{S_{33}^0} + \frac{\chi_{12}}{v_{12}} - \frac{2\chi_{13}}{v_{13}} - \frac{2\chi_{23}}{v_{23}} \tag{3}$$

dx.doi.org/10.1021/ma401665h | Macromolecules XXXX, XXX, XXX−XXX

in terms of the Flory–Huggins interaction parameters χ_{12}, χ_{13}, and χ_{23}, and the reference volumes $v_{12} = (v_1v_2)^{1/2}$, $v_{13} = (v_1v_3)^{1/2}$, and $v_{23} = (v_2v_3)^{1/2}$. The fully interacting system structure factors can be expressed as:

$$S_{11}(Q) = \frac{S_{11}^0(1 + V_{22}S_{22}^0)}{\Delta}$$

$$S_{22}(Q) = \frac{S_{22}^0(1 + V_{11}S_{11}^0)}{\Delta}$$

$$S_{12}(Q) = \frac{S_{11}^0(1 + V_{12}S_{22}^0)}{\Delta} \quad (4)$$

The denominator is given by $\Delta = (1 + V_{11}S_{11}^0)(1 + V_{22}S_{22}^0) - V_{12}^2S_{11}^0S_{22}^0$. The relation $\Delta = 0$ yields the spinodal condition. The SANS macroscopic scattering cross section (in units of cm^{-1}) is given by:

$$\frac{d\sum(Q)}{d\Omega} = (\rho_1 - \rho_3)^2S_{11}(Q) + (\rho_2 - \rho_3)^2S_{22}(Q) + 2(\rho_1 - \rho_3)(\rho_2 - \rho_3)S_{12}(Q) \quad (5)$$

Here ρ_1, ρ_2 and ρ_3 are the neutron scattering length densities.

For the PNIPAM/*d*-water/*d*-ethanol mixture, the following parameters were used

$$n_1 = 159.3, \quad n_2 = n_3 = 1$$

$$v_1 = 1.61 \times 10^{-22}cm^3, \quad v_2 = 3.0 \times 10^{-23}cm^3, \quad v_3 = 9.74 \times 10^{-23}cm^3$$

$$\rho_1 = 1.87 \times 10^{-7}Å^{-2}, \quad \rho_2 = 6.37 \times 10^{-6}Å^{-2}, \quad \rho_3 = 6.07 \times 10^{-6}Å^{-2} \quad (6)$$

Recall the component numbering: 1, PNIPAM; 2, *d*-water; 3, *d*-ethanol. The only remaining factor to determine is the single-chain form factor P(Q). The volume fractions of the three components are $\phi_1 = 0.034$, $\phi_2 = \phi_{dw}(1 - \phi_1)$ where ϕ_{dw} is the *d*-water relative fraction in the *d*-water/*d*-ethanol mixture and $\phi_3 = 1 - \phi_1 - \phi_2$. Since excluded volume interactions contribute in polymer solutions, a form factor which accounts for this parameter is employed.

Polymer With Excluded Volume. A model describing polymer chain conformations with excluded volume is used. The form factor for this model[17,18] is given by

$$P(Q) = 2\int_0^1 dx\,(1 - x)\exp\left[-\frac{Q^2a^2}{6}n^{2\nu}x^{2\nu}\right] \quad (7)$$

Here ν is the excluded volume parameter which is related to the Porod exponent m as $\nu = 1/m$, a is the polymer chain statistical segment length, n is the degree of polymerization, and x is the integration variable. This integral was performed[17] to yield:

$$P(Q) = \frac{1}{\nu U^{1/2\nu}}\gamma\left(\frac{1}{2\nu}, U\right) - \frac{1}{\nu U^{1/\nu}}\gamma\left(\frac{1}{\nu}, U\right) \quad (8)$$

Here, $\gamma(x,U)$ is the lower incomplete gamma function:

$$\gamma(x, U) = \int_0^U dt\,\exp(-t)t^{x-1} \quad (9)$$

The variable U is given in terms of the scattering variable Q as

$$U = \frac{Q^2a^2n^{2\nu}}{6} = \frac{Q^2R_g^{\,2}(2\nu + 1)(2\nu + 2)}{6} \quad (10)$$

The radius of gyration squared has been defined as

$$R_g^{\,2} = \frac{a^2n^{2\nu}}{(2\nu + 1)(2\nu + 2)} \quad (11)$$

Note that fully swollen chains have a Porod exponent of 5/3 (good solvent), Gaussian chains have a Porod exponent of 2 (Θ solvent) while collapsed chains have a Porod exponent of 3 (bad solvent).[19]

Flory–Huggins Interaction Parameters and Radius of Gyration. Using the ternary RPA model developed in the previous sections, SANS data were analyzed for each temperature and each *d*-water/*d*-ethanol fraction (i.e., ϕ_{dw}). The varying fitting parameters are R_g, ν, and the incoherent background B along with the three Flory–Huggins interaction parameters $\chi_{12}(T,\phi_{dw})$, $\chi_{13}(T,\phi_{dw})$, and $\chi_{23}(T,\phi_{dw})$. The $1/T$ dependence is made explicit by splitting $\chi_{ij}(T,\phi_{dw}) = E_{ij}(\phi_{dw}) + F_{ij}(\phi_{dw})/T$ for all three χ parameters. The inverse solvation intensity $1/C$ (shown in Figure 5) is characterized by a parabolic dependence on ϕ_{dw}. This suggests the following separation $E_{ij}(\phi_{dw}) = A_{ij} + B_{ij}\phi_{dw}^{\,2}$ and $F_{ij}(\phi_{dw}) = C_{ij} + D_{ij}\phi_{dw}^{\,2}$ for a total of 12 χ-related varying parameters, but with a large number of SANS data points (Q-dependent scattering intensity) to constrain possible parameters.

Since the right branch of the phase diagram ($0.8 \le \phi_{dw} \le 1$) contains interference from the low-Q signal in SANS data (as shown in Figure 4) separating the solvation feature (intermediate and high-Q signal) is difficult, especially for $T \ge 25$ °C. Thus, emphasis will be made on the left branch of the phase diagram ($0 \le \phi_{dw} \le 0.04$).

Figure 7 shows the variation of the three χ parameters with increasing ϕ_{dw} fraction. One can see that χ_{12} decreases while χ_{13} and χ_{23} increase. Smooth lines are drawn though the data as

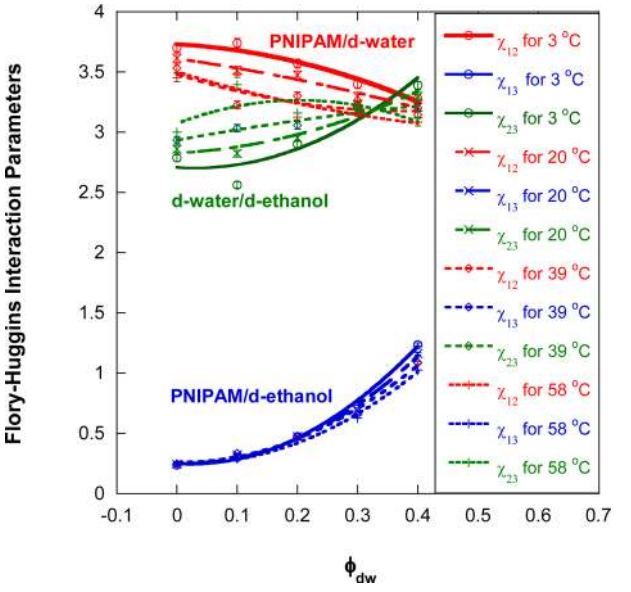

Figure 7. Variation of the three Flory–Huggins interaction parameters for increasing *d*-water fraction and for four sample temperatures (3, 20, 39, and 58 °C). The components are numbered as follows: 1, PNIPAM; 2, *d*-water; 3, *d*-ethanol. Statistical error bars correspond to one standard deviation.

dx.doi.org/10.1021/ma401665h | Macromolecules XXXX, XXX, XXX–XXX

guides to the eye. Note the highly nonlinear dependence of the χ parameters on composition ϕ_{dw}.

The same parameters are plotted in parts a and b of Figure 8 for increasing $1/T$. The interaction parameter between water and ethanol cannot be obtained from SANS in the limiting cases of pure water or pure ethanol solvents. These points in Figures 7 and 8 are instead obtained by extrapolation. Note that for the limiting cases of 0% *d*-water and 100% *d*-water, the binary RPA model predicts that a negative slope with respect to $1/T$ indicates LCST behavior, while a positive one indicates UCST behavior. This simple rule does not hold for ternary mixtures with composition-dependent parameters. Note for example, that in the left branch of the phase diagram ($\phi_{dw} \leq 0.4$) χ_{12} (PNIPAM/*d*-water) has a positive slope, yet for $\phi_{dw} = 1$, it has a negative slope. For these values, χ_{13} has a mostly positive slope. It is interesting to note that the χ_{23} (*d*-water/*d*-ethanol) parameter also has a negative slope with low *d*-water content, and then switches to a positive slope when water content increases. However, the $1/T$ dependence of χ is maintained throughout the range of measured temperatures.

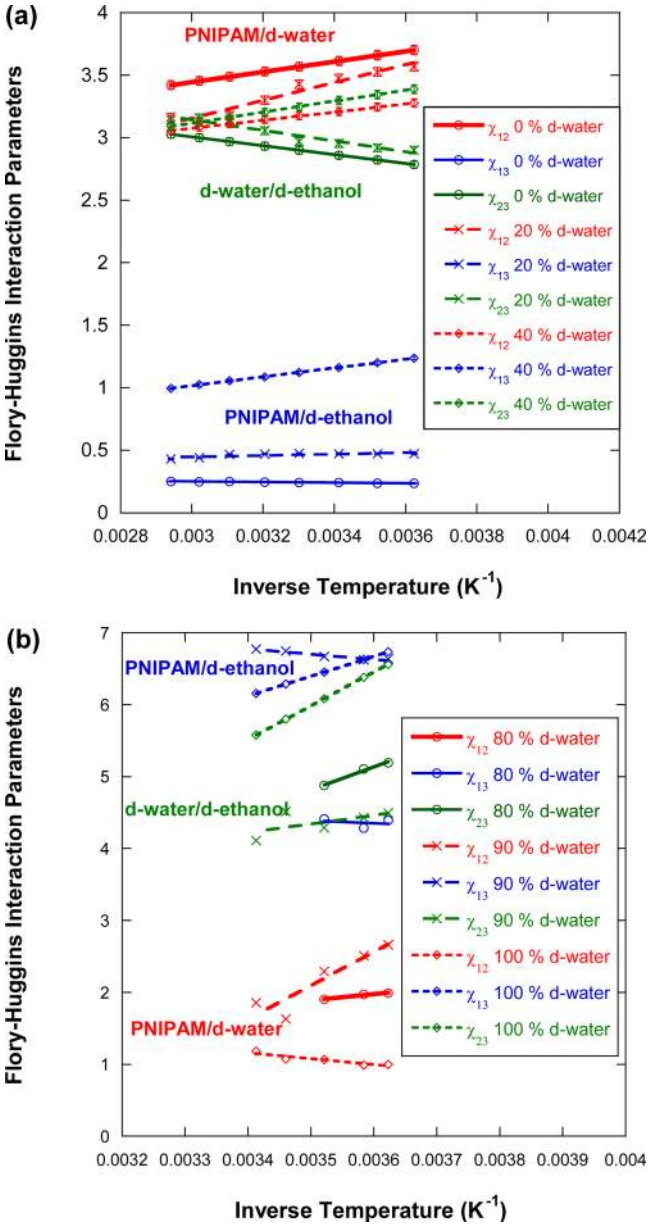

Figure 8. Variation of the three Flory–Huggins interaction parameters with 1/T for three *d*-water fractions for (a) the left branch of the phase diagram ($\phi_{dw} \leq 0.4$) and (b) for the right branch of the phase diagram ($0.8 \leq \phi_{dw} \leq 1$). Statistical error bars correspond to one standard deviation.

Figure 9 summarizes the fit results for the radius of gyration R_g and its variation with temperature. Polymer coils tend to swell for increasing temperature for the low *d*-water fractions. For the 40% *d*-water fraction polymer chains shrink instead. R_g shows an interesting trend reversal. This effect is real and well outside of fitting statistics.

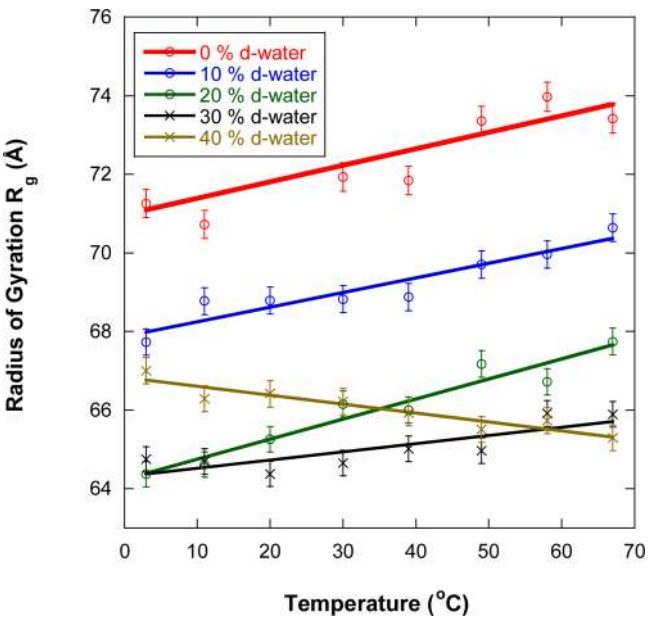

Figure 9. Variation of the radius of gyration with increasing temperature for the various *d*-water fractions. Statistical error bars correspond to one standard deviation.

DISCUSSION

SANS measurements reproduce and extend the phase diagram (*cf.*, Figure 6) determined by Costa and Freitas[11] using cloud point measurements for PNIPAM in solvent mixtures of water and ethanol. The behavior of PNIPAM in ethanol and propanol is quite different from that of PNIPAM in water and methanol, which exhibits only LCST behavior. A particular finding of Costa and Freitas is that as the hydrophobic portion of the alcohol increases, as in moving from methanol to ethanol, the structure of the alcohol competes with hydrogen bonding between the water molecules and hydroxyl group of the alcohol. Thus, as the amount of water increases, ethanol becomes confined to hydration structures and cannot interact with the PNIPAM chain, which has been suspected to interact more favorably with ethanol than water.

The analysis of SANS data using the ternary RPA model provides additional insight into the thermodynamics that govern the behavior of PNIPAM in solvent mixtures. In particular, Figures 7 and 8 provide information regarding the interaction of PNIPAM with water (red) and ethanol (blue), as well as the interaction between water and ethanol (green). Figure 7 demonstrates that for *d*-water fractions up to 40%, the Flory–Huggins interaction parameter between *d*-ethanol and

dx.doi.org/10.1021/ma401665h | Macromolecules XXXX, XXX, XXX–XXX

PNIPAM is smaller in magnitude than that for PNIPAM and water, as speculated by Costa and Freitas[11] and Mukae et al.[20] Hence, PNIPAM and ethanol interactions are energetically favored as compared to PNIPAM/*d*-water or *d*-water/*d*-ethanol interactions. Furthermore, while the PNIPAM and *d*-ethanol interaction increases as ϕ_{dw} increases, it remains much smaller in magnitude than the interaction parameters between the other components. In addition, the interaction parameters for PNIPAM/*d*-water and *d*-water/*d*-ethanol display a nontrivial behavior with respect to water content as compared to PNIPAM/*d*-ethanol. We speculate that this behavior may be due, in part, to a competition between the formation of *d*-water/*d*-ethanol complexes (e.g., hydration structures) and solvation of the PNIPAM chains. For example, spectroscopy[21] and molecular dynamics simulations[22] have established that the local structure of the hydrogen bonding network of water around ethanol depends strongly upon the mole fraction of water present. Molecular dynamics simulations by Pang et al. found PNIPAM interactions with mixed methanol/water solvents weaken as methanol is added.[23] Thus, it may be that at certain compositions of the solvent mixture, interaction of the solvent with itself is favored over interaction with the polymer chains, giving rise to the nonlinear behavior presented in Figure 7. Nevertheless, the origin of the nonlinear behavior of the interaction parameters with respect to *d*-water content is not understood from a molecular perspective presently, and remains a topic for future investigation, for example, by systematic molecular dynamics simulations.

The behavior of the PNIPAM radius of gyration, Figure 9, is in good agreement with trends measured by Zhang and Wu[9,24] for PNIPAM in water/methanol mixtures. The values of R_g are also in accord with recent SANS and light scattering measurements of a PNIPAM with similar molecular weight in water.[25] Interestingly, R_g increases at 0 °C as φ_{dw} increases from 30% to 40%. The increase in R_g observed for 40% *d*-water (0 °C) may be due to clustering of PNIPAM chains in solution. However, the increase is small (less than 1 nm), and lower than what would be expected for clusters of several chains, implying that this is unlikely the source of the increase. In general, however, PNIPAM chains are found to shrink as *d*-water is added to the system, and expand as T increases away from the spinodal line, as predicted and previously measured.[9,24]

SUMMARY

The PNIPAM polymer has decidedly unusual behavior in many ways. Most water-soluble polymers dissolve better in solvent mixtures. However, the PNIPAM polymer behaves differently. Some solvent mixtures are worse at dissolving PNIPAM than the individual solvents themselves. Using the SANS technique, the phase behavior of a dilute PNIPAM solution in *d*-ethanol/*d*-water mixtures was investigated. The mixing/demixing phase diagram shows a region dominated by the UCST behavior in the *d*-ethanol rich branch and a region dominated by the LCST behavior in the *d*-water rich branch of the phase diagram. The region in-between is dominated by cononsolvency where the polymer does not dissolve.

A ternary random phase approximation model is used to analyze SANS data. A polymer form factor that incorporates chain swelling/shrinking is used to better represent chain conformations in solution. The three Flory–Huggins interaction parameters $\chi_{PNIPAM/d-water}$, $\chi_{PNIPAM/d-ethanol}$, and $\chi_{d-water/d-ethanol}$ were obtained. These display the usual $1/T$ behavior as well as a strong dependence on *d*-water fraction ϕ_{dw}. This strong dependence on *d*-water fraction remains an open topic for future investigation. Slopes of the χ vs $1/T$ variation depend on the *d*-water fraction; these could be either positive or negative. The proper slopes are recovered for the binary mixtures limits; the PNIPAM/*d*-ethanol parameter corresponds to UCST trend (phase separation upon cooling) while the PNIPAM/*d*-water parameter corresponds to LCST phase separation trend (phase separation upon heating). The radius of gyration is observed to increase for increasing temperature at low *d*-water fractions. This trend reverses close to the boundary of the left branch of the phase diagram (i.e., for $\phi_{dw} = 0.4$).

The various trends in the radius of gyration and Flory–Huggins interactions parameters, obtained from the analysis of SANS data, point to an intricate solvation behavior and interplay of the two solvents around the polymer. SANS indicates that solvent mixing is far from random but cannot determine the structure of solvent molecules around the polymer. The binary mixture of PNIPAM in pure *d*-water does not follow a simple demixing behavior as temperature is increased, and will be the subject of future investigations. Furthermore, the nonlinear variation of the Flory–Huggins interaction parameters with *d*-water content warrants further investigation by atomistic molecular dynamics, for example.

AUTHOR INFORMATION

Corresponding Authors

*(M.J.A.H.) E-mail: michael.hore@nist.gov.
*(B.H.) E-mail: hammouda@nist.gov.
*(H.C.) E-mail: chenghe@iccas.ac.cn.

Notes

The authors declare no competing financial interest.

ACKNOWLEDGMENTS

The identification of commercial products does not imply endorsement by the National Institute of Standards and Technology nor does it imply that these are the best for the purpose. This work is based upon activities supported in part by the National Science Foundation under Agreement No. DMR-0944772. M.J.A.H. was supported by a National Research Council (NRC) postdoctoral fellowship at the NIST Center for Neutron Research. H.C. was supported by the National Natural Scientific Foundation of China (No. 21174152). Helpful discussions with Nitash Balsara and Charles Han are appreciated.

REFERENCES

(1) Hammouda, B. *Probing Nanoscale Structures – The SANS Toolbox*, Chapter 54, http://www.ncnr.nist.gov/staff/hammouda/the_sans_toolbox.pdf
(2) Wolf, B. A.; Willms, M. M. *Makromol. Chem.* **1978**, *179*, 2265–2277.
(3) Young, T. H.; Tao, C. T.; Lai, P. S. *Polymer* **2003**, *44*, 1689–1695.
(4) Guettari, M.; Gomati, R.; Gharbi, A. *J. Macromol. Sci., Part B* **2010**, *49*, 552–562.
(5) Takahashi, N.; Kanaya, T.; Nishida, K.; Kaji, K. *Polymer* **2003**, *44*, 4075–4078.
(6) Kirotsu, S. *J. Chem. Phys.* **1988**, *88*, 427.
(7) Winnik, F. M.; Ringsdorf, H.; Venzmer, J. *Macromolecules* **1990**, *23*, 2415–2416.
(8) Schild, H. G.; Muthukumar, M.; Tirrell, D. A. *Macromolecules* **1991**, *24*, 948–952.
(9) Zhang, G.; Wu, C. *J. Am. Chem. Soc.* **2001**, *123*, 1376–1380.

(10) Tucker, A. K.; Stevens, M. J. *Macromolecules* **2012**, *45*, 6697−6703.
(11) Costa, R. O. R.; Freitas, R. F. S. *Polymer* **2002**, *43*, 5879−5885.
(12) Yamauchi, H.; Maeda, Y. *J. Phys. Chem. B* **2007**, *111*, 12964−12968.
(13) Tanaka, F.; Koga, T.; Winnik, F. M. *Phys. Rev. Lett.* **2008**, *101*, 028302.
(14) Convertine, A. J.; Lokitz, B. S.; Vasileva, Y.; Myrick, L. J.; Scales, C. W.; Lowe, A. B.; McCormick, C. L. *Macromolecules* **2006**, *39*, 1724.
(15) Bauri, K.; Roy, S. G.; Arora, S.; Dey, R. K.; Goswami, A.; Madras, G.; De, P. *J. Therm. Anal. Calorim.* **2013**, *111*, 753.
(16) Akcasu, A. Z.; Tombakoglu, M. *Macromolecules* **1990**, *23*, 607−612.
(17) Hammouda, B. *Adv. Polym. Sci.* **1993**, *106*, 87−133.
(18) Benoit, H. *Comptes Rendus.* **1957**, *245*, 2244−2247.
(19) Flory, P. *Principles of Polymer Chemistry*; Cornell University Press: Ithaca, NY, 1953.
(20) Mukae, K.; Sakurai, M.; Sawamura, S.; Makino, K.; Kim, S. W.; Ueda, I.; Shirahama, K. *J. Chem. Phys.* **1993**, *97*, 737.
(21) Pradhan, T.; Ghoshal, P.; Biswas, R. *J. Chem. Sci.* **2008**, *120*, 275−287.
(22) Zhang, C.; Yang, X. *Fluid Phase Equilib.* **2005**, *231*, 1−10.
(23) Pang, J.; Yang, H.; Ma, J.; Cheng, R. *J. Phys. Chem. B* **2010**, *114*, 8652−8658.
(24) Zhang, G.; Wu, C. *Phys. Rev. Lett.* **2001**, *86*, 822.
(25) Nishi, K.; Hiroi, T.; Hashimoto, K.; Fujii, K.; Han, Y.-S.; Kim, T.-H.; Katsumoto, Y.; Shibayama, M. *Macromolecules* **2013**, *46*, 6225−6232.